

Supporting Information

Aptamer-functionalized nanoscale metal-organic frameworks for targeted photodynamic therapy

Hong-Min Meng,^{†a} Xiaoxiao Hu,^{†b} Ge-Zhi Kong,^b Chan Yang,^b Ting Fu,^b Zhao-Hui Li,^{*a} and Xiao-Bing Zhang^{*b}

^a Henan Joint International Research Laboratory of Green Construction of Functional Molecules and Their Bioanalytical Applications, College of Chemistry and Molecular Engineering, Zhengzhou University, Zhengzhou 450001, P. R. China.

^b Molecular Sciences and Biomedicine Laboratory, State Key Laboratory for Chemo/Biosensing and Chemometrics, College of Chemistry and Chemical Engineering, Collaborative Innovation Center for Chemistry and Molecular Medicine, Hunan University, Changsha 410082, P. R. China.

* To whom correspondence should be addressed.

zhaohui.li@zzu.edu.cn; xbzhang@hnu.edu.cn

Supporting table and figures

Table S1. Sequences of Oligonucleotides Used in This Work

Oligonucleotide	Sequences (from 5' to 3')
G4-sgc8 (FAM)	PO ₄ ³⁻ -TGG GGT TTT GGG GTT TTA TCT AAC TGC TGC GCC GCC GGG AAA ATA CTG TAC GGT TAG A-FAM
G4-sgc8	PO ₄ ³⁻ -TGG GGT TTT GGG GTT TTA TCT AAC TGC TGC GCC GCC GGG AAA ATA CTG TAC GGT TAG A
Sgc8 (FAM)	ATC TAA CTG CTG CGC CGC CGG GAA AAT ACT GTA CGG TTA GA-FAM
Lib (FAM)	ACC TGG GGG AGT AAA AAA AAA AAA AAA AAA AAA AAA AAA AA-FAM

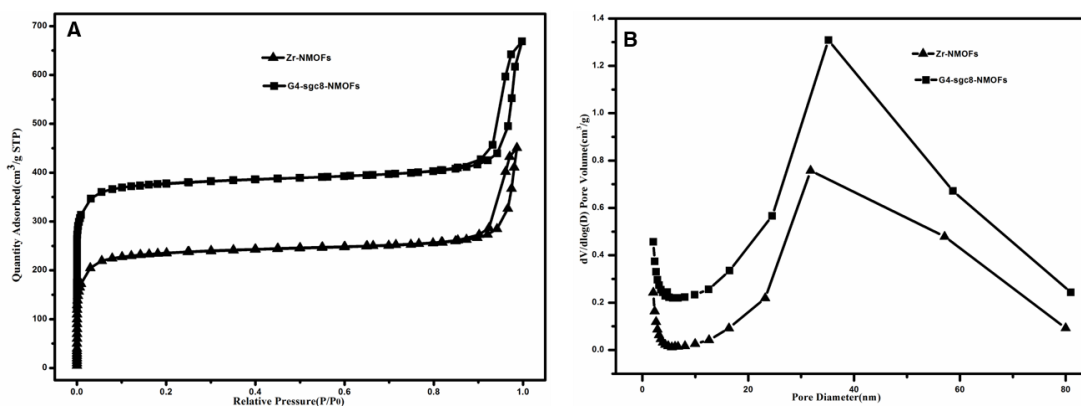


Figure S1. (A) N₂ adsorption-desorption isotherms and (B) the corresponding pore-size distribution curve of Zr-NMOFs and G4-sgc8-NMOFs.

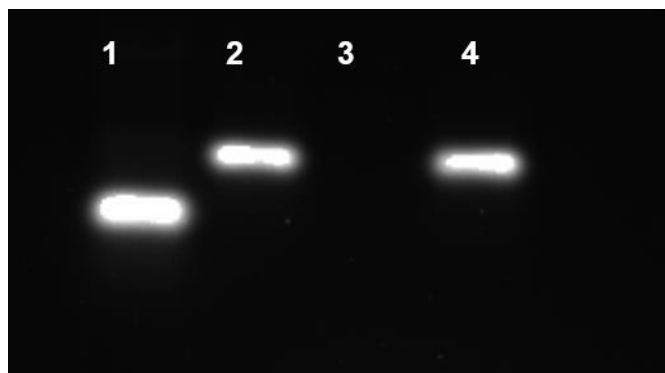


Figure S2. Agarose gel electrophoresis tests of the G4-sgc8 (lane 1), G4-sgc8-NMOFs (lane 2), G4-sgc8 treated with serum for 8 h (lane 3) and the G4-sgc8-NMOFs treated with serum for 8 h (lane 4).

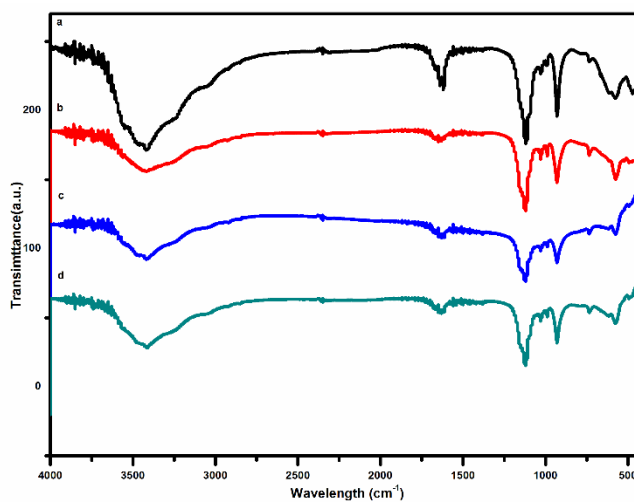


Figure S3. FTIR spectra of the samples of (a) G4-sgc8, (b) TMPyP4, (c) TMPyP4-G4-sgc8, (d) TMPyP4-G4-sgc8-NMOFs.

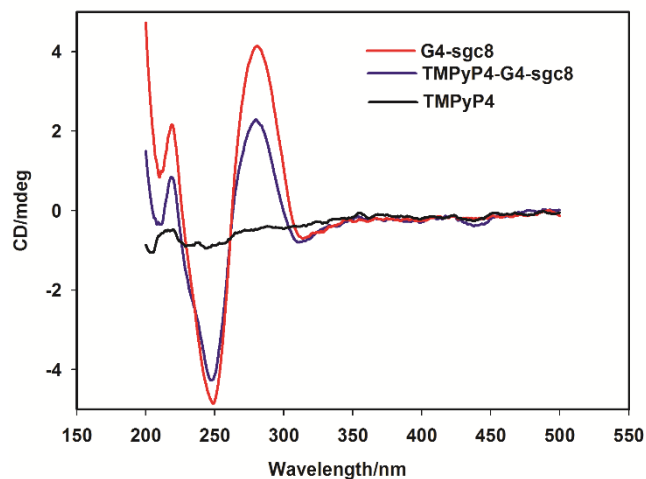


Figure S4. CD spectra of TMPyP4, the G4-sgc8, and the TMPyP4-G4-sgc8 (G4-sgc8=10 μ M).

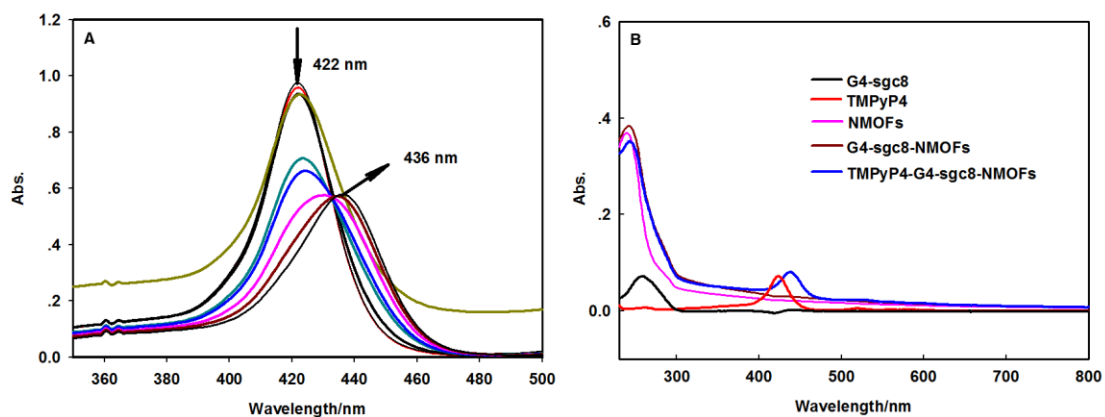


Figure S5. (A) UV/Vis absorption spectra of TMPyP4 (4 μ M) with the different concentrations (0, 0.05, 0.1, 0.15, 0.2, 0.3, 0.4, 0.5, 0.6, 0.8 μ M) of G4-sgc8. (B) UV/Vis absorption spectra of G4-sgc8 (0.4 μ M), TMPyP4 (2 μ M), NMOFs (100 μ g/mL), G4-sgc8-NMOFs (100 μ g/mL) and TMPyP4-G4-sgc8-NMOFs (100 μ g/mL).

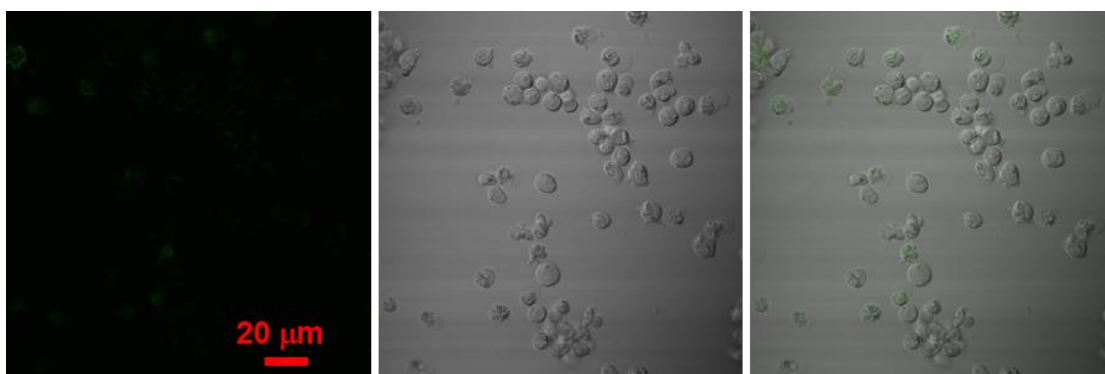


Figure S6. Confocal laser-scanning microscopy imaging of Ramos cells treated with 100 μ g/mL G4-sgc8-NMOFs.

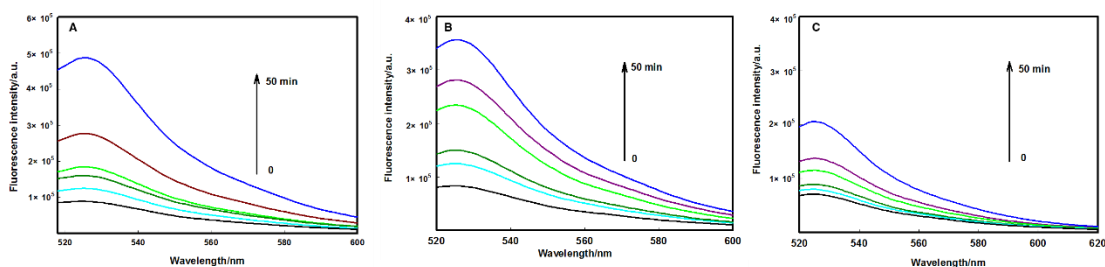


Figure S7. Determination of singlet oxygen through the strong fluorescence of singlet oxygen sensor green (SOSG) upon oxidation by singlet oxygen with different light sources. (A) 405nm laser, (B) white light and (C) 660nm laser.

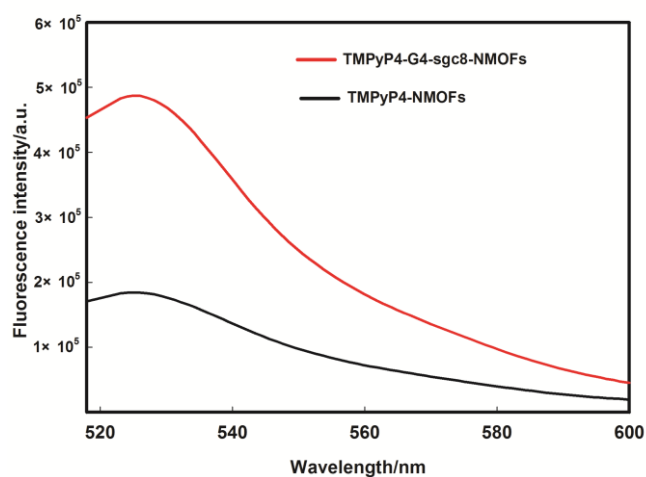


Figure S8. Determination of singlet oxygen through the strong fluorescence of singlet oxygen sensor green (SOSG) upon oxidation by 405nm laser.

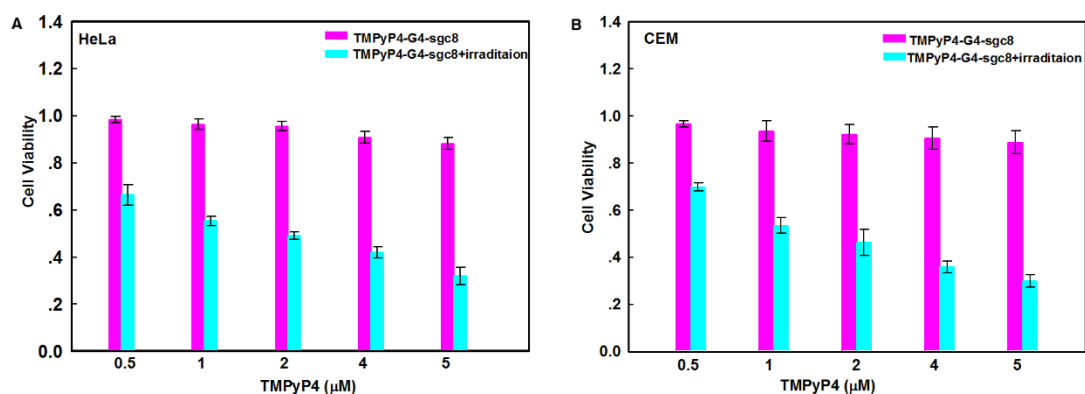


Figure S9. Cytotoxicity of TMPyP4-G4-sgc8 at different concentrations in the presence or absence of irradiation for HeLa and CEM cells.

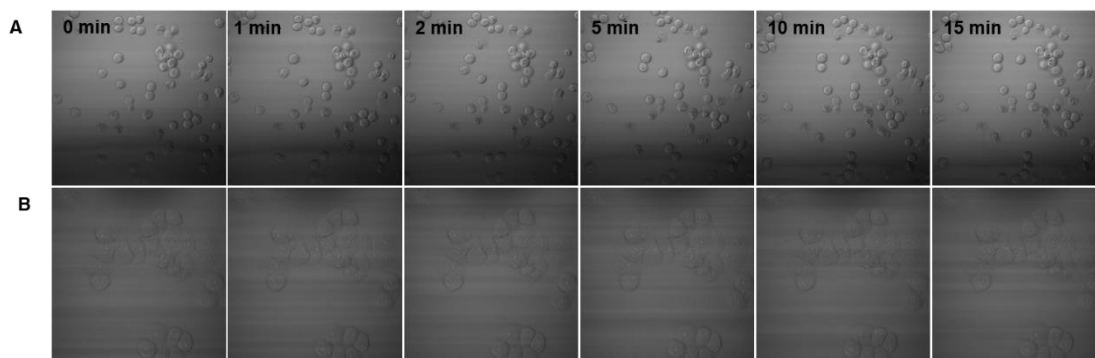


Figure S10. Real-time morphology of (A) Ramos cells treated with TMPyP4-G4-sgc8-NMOFs nanosystem and (B) HeLa cells under laser at 405 nm.

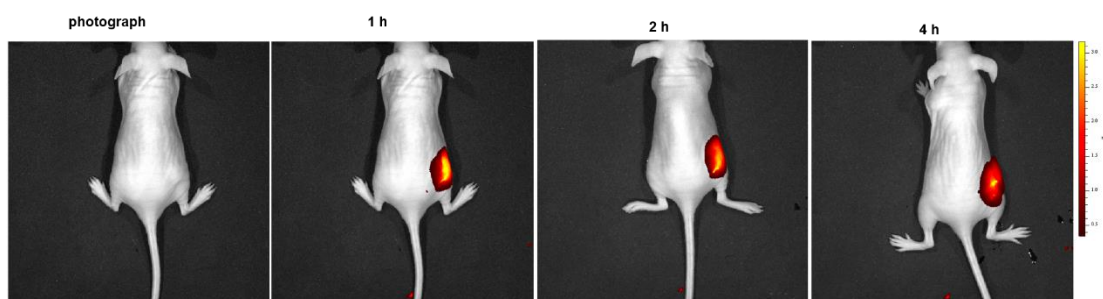


Figure S11. Time-dependent in vivo fluorescence images of tumor-bearing mice after intratumoral injection of TMPyP4-G4-sgc8-NMOFs.